2-D PIC Simulation on Electron Sheath Formation in Magnetized Plasmas

Kazuhito ASANO[1], Shin KAJITA[2], Dai OIKAWA[3] and Noriyasu OHNO[3]

[1]*Japan NUS Co., Ltd., 15-9 Kaigan 3, Minato, Tokyo, 108-0022, Japan,*

[2]*EcoTopia Science Institute of Nagoya University, Furo-Chou, Chikusa, Nagoya, 464-8603, Japan,*

[3]*Department of Energy Engineering and Science, Graduate School of Engineering, Nagoya University, Furo-Chou, Chikusa, Nagoya, 464-8603, Japan*

(Received: 29 October 2009 / Accepted: 5 March 2010)

In order to analyze electron sheath formation we performed two dimensional PIC (Particle In Cell) simulations in magnetized plasmas. We investigated the influence of the probe geometry on the electron sheath formation in terms of the aspect ratio of the plane probe. The dependence of the magnetic field and voltage bias of the probe on the electron sheath were also taken into consideration. The sheath thickness was also analyzed to compare with the theoretical formula described by the Child Langmuir (CL) law and the experimental observations. We found that alteration of the plane probe geometry from rectangular to square decreased sheath thickness, resulting in a close to cylindrical CL sheath, rather than a planar one. These results demonstrate that the behavior of electrons surrounding the probe is directly affected by the geometry of the probe. Further, it is found that the sheath thickness is determined by the ratio between the probe width and the Larmor radius of the electron.

Keywords: electron sheath, Particle In Cell, Child Langmuir law, magnetized plasmas, angular momentum of electron, cylindrical effect

1. Introduction

There have been various studies about the influence of a magnetic field on ion sheath formation, both experimentally and numerically [1]. There are few studies, however, on the influence of the magnetic field on the electron sheath formation. The study reported here provides a detailed analysis of the electron sheath formation around the electrostatic probe biased positively with respect to plasma potential.

The thickness of the electron sheath that forms around a planar or cylindrical probe was measured experimentally in weakly magnetized plasmas, using the laser photodetachment (LPD) technique [2,3]. These studies show that the electron sheath thickness is sensitive to the magnetic field as well as the geometry of the probe.

In order to perform a detailed analysis on the influence of the magnetic field and the geometry of the probe on the electron sheath formation, we employed PIC simulation code, called XOOPIC [4]. XOOPIC supports two dimensional space, slab and cylindrical geometries and has electrostatic and electromagnetic solvers. PIC simulation determines the electric and magnetic fields self-consistently for various boundary conditions and plays a key role in the analysis and understanding of electron sheath formation.

In this paper we report a detailed analysis of the two dimensional electron sheath structure formed around a probe using a PIC simulation, where the electrostatic solver is applied. We further evaluate and discuss the validity of the Child-Langmuir (CL) formula for accurate prediction of electron sheath thickness.

author's e-mail:asano@janus.co.jp

2. Simulation setup

Figure 1 shows a schematic view of the simulation setup. The plane probe, biased positively, is located at the center of the region along the magnetic field. Each boundary is fixed at 0 V and hydrogen plasma is injected from boundary with half-Maxwellian velocity distribution. Electron and ion density, n_e and n_i are set to be $10^{17}\mathrm{m}^{-3}$ and

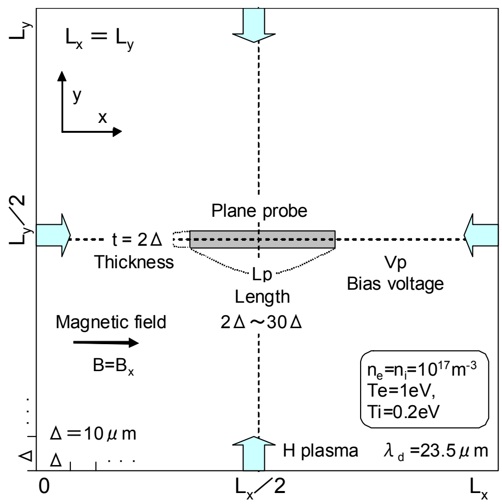

Variable Parameter	
Bx	1 ～ 100mT
Vp	30 ～ 120V
Lp:t	30:2 ～ 2:2

Fig.1 Simulation model and plasma parameters.

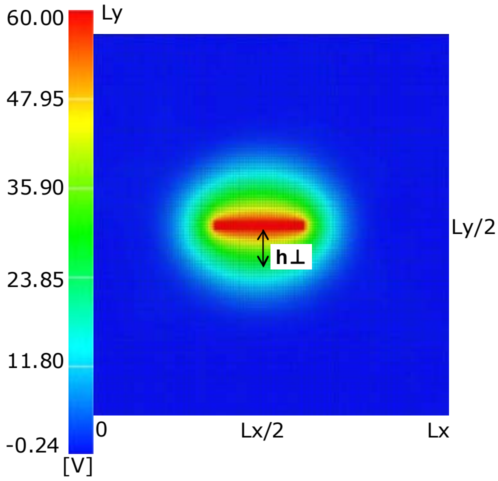

Fig.2 A potential profile and the schematic image of calculated sheath thickness in B=1 mT, V_p=60V and L_p:t=30:2. The steady state potential profile is averaged over 0.7 μs～1.1 μs or 2000f_{pe}^{-1}～3142f_{pe}^{-1}, where f_{pe} is the electron plasma frequency.

temperature, Te and Ti are 1eV and 0.2eV respectively. Debye length, λd is calculated to be 23.5 μm. The length of the simulation region, L, is large enough not to affect the sheath. The validity of L is confirmed by checking potential profile, which is approximately 0V in a region that is far from electrode. This is achieved at a distance of L > 1mm.

To investigate the effect of the probe geometry on sheath thickness, various aspect ratios are assessed by adjusting the width of the plane probe as shown in Fig.1. The static magnetic field applied in the x direction and the bias voltage of the plane probe V_p were varied from 1 mT to 100 mT and 30 V to 120 V, respectively.

A steady state potential profile can be obtained as shown in Fig.2. The sheath thickness, $h_\perp$, is evaluated by using this potential profile as follows. The potential of the sheath edge is defined such that, $V_{edge} = V_p / exp$, where *exp* is an *base of natural* logarithm. We are able to determine the position, whose potential corresponds to V_{edge} for vertical direction, in the magnetic field at the center of probe as, $y(V_{edge})_{x=Lx/2}$. Subsequently $h_\perp$ is calculated using following formula.

$$h_\perp = y(V_p)_{x=L_x/2} - y(V_{edge})_{x=L_x/2} \tag{1}$$

Figure 2 shows an example of the calculation of sheath thickness, where V_{edge} is calculated to be 60/*exp* ～22V where V_p= 60 V.

3. Simulation results

Theoretically, the electron sheath thickness obeys the CL law such that the thickness of the CL sheath formed in front of a planar electrode, h_p, or that of a the cylindrical electrode, h_c, can be written as follows [5],

$$h_p = \frac{2}{3}\sqrt{-\frac{\varepsilon_0}{j}}\left(\frac{2e(V_p - V_{sp})^3}{m_e}\right)^{1/4}, \text{ and} \tag{2}$$

$$h_c = -\frac{8\pi\varepsilon_0}{9j\beta^2}\sqrt{\frac{2e}{m_e}}(V_p - V_{sp})^{3/2}, \tag{3}$$

where V_{sp} is the space potential, e is the elementary charge and $\beta = f\left((r_p + h_c)/r_p\right)$, r_p is the probe tip radius. The f is a function as radius given numerically [5]. These equations indicate that the CL sheath in the cylindrical geometry has stronger dependence on the electron current

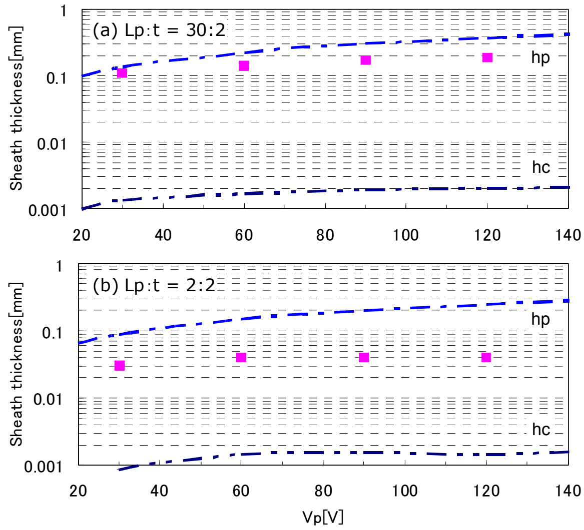

Fig.3 The thickness of the electron sheath formed around the plane probe. (a) corresponds to Lp:t=30:2 (rectangle electrode) and (b) corresponds Lp:t=2:2 (square electrode), in B=15mT for each case. Lp is length of electrode for x direction and t is thickness for y direction.

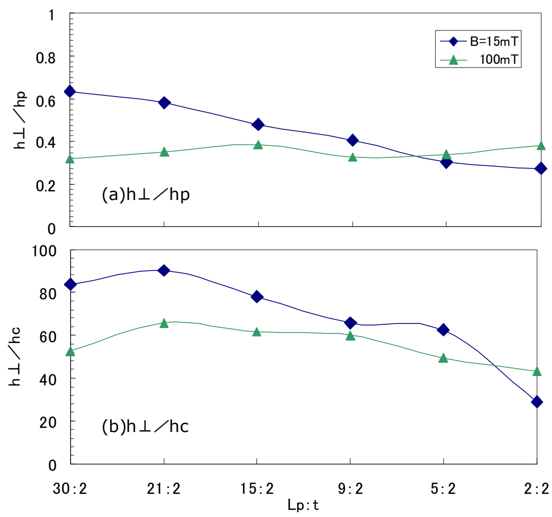

Fig.4 Ratio of sheath thickness to (a) plane CL sheath and (b) cylindrical CL sheath at different aspect ratio. V_p is set to be 60V.

density j than CL sheath in plane-parallel one depicted in Fig.1. This means that a cylindrical probe has a greater capability for collection of an electron current.

Figure 3 shows the sheath thickness at different bias voltages of the probe in B=15mT. It can be seen, from Fig.3 (a), that the sheath thickness calculated by simulation is approximately equal to h_p under a high aspect ratio, where Lp:t=30:2. On the other hand, as shown in Fig.3(b), the sheath thickness is close to h_c under a low aspect ratio where, Lp:t=2:2. This clearly indicates that the geometry of the plane probe significantly influences the behavior of electrons around the probe resulting in a change in the potential profile around the probe which leads to a decrease in the sheath thickness. This also indicates that a low aspect ratio has more electron collective effect than rectangle one as well as cylindrical geometry.

The ratio of sheath thickness to CL sheath, at different aspect ratios is analyzed as shown in Fig.4. This figure shows that sheath thickness in weakly magnetized plasma has stronger dependence on the aspect ratio than strongly magnetized. The sheath thickness decreases as the aspect ratio decreases in weakly magnetized plasma and close to CL sheath in the cylindrical geometry.

4. Discussion

4.1 Geometric effect of plane probe

Figure 5 shows the distribution of electron and ion. This figure suggests that the electrons are condensed, in case of low aspect ratio and shield the electric field. In Fig. 5(b), the turn of electron around probe is observed due to its angular momentum. Fig.6 shows a schematic drawing of the effect of the angular momentum of electron. The

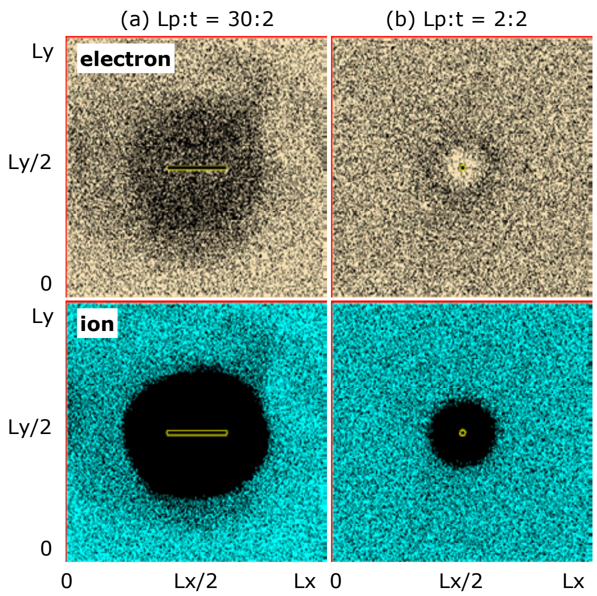

Fig.5 Distribution of electron and ion to show the effect of aspect ratio of plane probe, Lp:t is (a) 30:2 and (b) 2:2, respectively. The magnetic field is set to be 1mT.

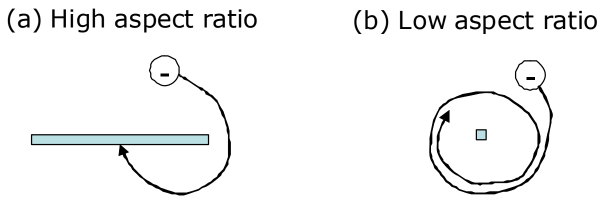

Fig.6 Schematic view of geometric effect. (a): electron vanishes after incidence of collision with electrode. (b): electron turns around electrode due to its angular momentum rather than incidence of collision. This is caused by electric field around electrode and angular momentum of electron.

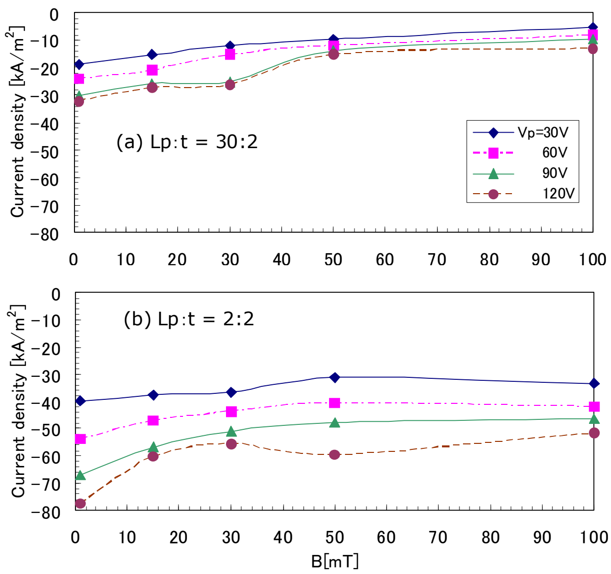

Fig.7 Current density of electron to the probe at different aspect ratio, (a) high aspect ratio and (b) low aspect ratio.

angular momentum of the electron results in an increase in electron density around the probe, which in turn shields the electric field, due to a decreased incidence of collisions between electron and the probe. In order to characterize the effect of the shielding effect due to angular momentum of the electron, the current density j, with different magnetic fields and bias voltage were plotted in Fig.7. The aspect ratio corresponds to Lp:t=30:2 in Fig.7(a) and 2:2 in Fig.7(b), respectively. It was revealed that the current density increases negatively as the aspect ratio decreases. This indicates that the collective ability of the electron current or the cylindrical effect is dominant in a low aspect ratio. This cylindrical effect makes the sheath thickness smaller than the CL sheath in plane parallel geometry as predicted by CL sheath in cylindrical one, shown in Eq. (2). As can be seen, a cylindrical effect, due to the effect of angular momentum of electrons, is produced on the plane probe by decreasing the aspect ratio.

4.2 Effect of magnetic field on sheath formation

Figure 8 shows the ratio of sheath thickness to CL sheath in plane parallel geometry at different magnetic fields and bias voltages. In Fig.8 (a), using a high aspect ratio, at the sheath thickness peaks around B=30mT. Conversely, as in the case of a low aspect ratio, no peak is observed as shown in Fig.8 (b).

The physical reason for these differential dependencies of the magnetic field on the sheath thickness could be effected by the considering the relationship between the probe width and the Larmor radius of the electron. In order to understand this phenomenon, we define the following index, L_e.

$$L_e = \langle v \rangle T_C / 2 \qquad (4)$$

$$\langle v \rangle = \sqrt{\frac{8kT_e}{\pi m_e}}, T_C = \frac{2\pi m_e}{eB},$$

where kT_e is the electron temperature in J. $\langle v \rangle$ is a random velocity of the electron and , T_c^{-1} is a cyclotron frequency. L_e means the distance an electron moves in half a Larmor motion. The relation between L_e and L_p, or aspect ratio, characterizes sheath formation.

Figure 9 shows the schematic view of the magnetic field effect on the Larmor motion of electrons to demonstrate the dependency of sheath formation on the Larmor motion of an electron. Three cases are considered. Case (a) where Larmor radius is small ($L_e < L_p$) and Case (b) $L_e \sim L_p$ and Case (c) $L_e > L_p$. In Case (c), an electron could likely cross the probe due to the larger Larmor radius. In Case (b), L_e is comparable to L_p, thus electrons would have a tendency to collide before crossing the probe. These behaviors are slightly different from each other but an impact on the sheath formation is comparable

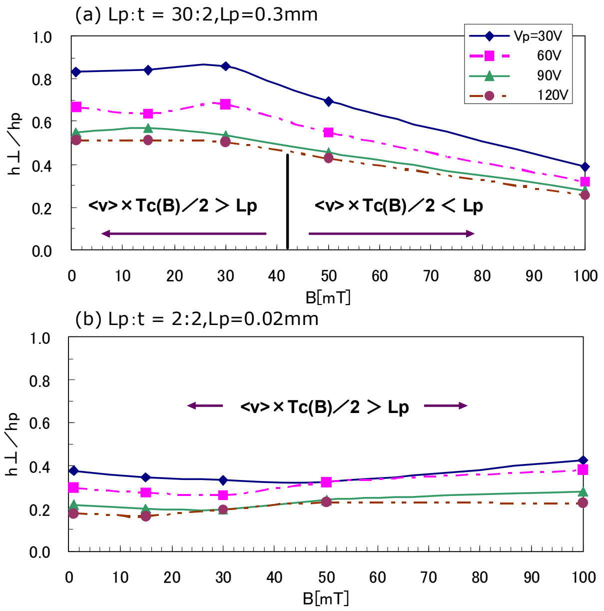

Fig.8 The ratio of sheath thickness to CL sheath in plane parallel geometry at different magnetic field, (a) high aspect ratio and (b) low aspect ratio. $\langle v \rangle$ is a random velocity of the electron, *Tc* is a cyclotron period.

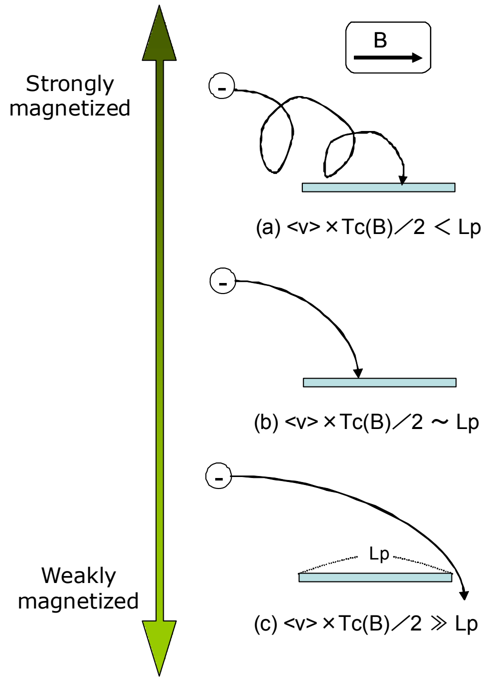

Fig.9 The schematic view of the magnetic field effect when the Larmor radius is (a) very small, (b) comparable with the probe width and (c) large enough.

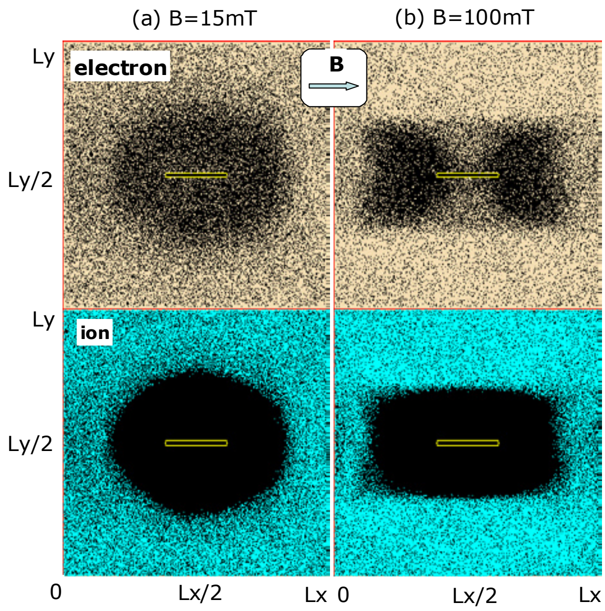

Fig.10 Distribution of electron and ion to show the effect of the magnetic field. In (a) B=15mT, and in (b) B=100mT. The bias voltage and the aspect ratio are set to be 60V and Lp:t=30:2, respectively.

in both cases. Finally, in Case (a), an electron can move close to the probe resulting in a potential profile around the probe that decreases as the Larmor radius decreases, or the magnetic field increases. In case of the high aspect ratio shown in Fig.8 (a), L_e is comparable with L_p in B$\sim$ 40mT. On the other hand, L_e is always greater than L_p in case of the low aspect ratio as shown in Fig.8 (b). These results agree with the relation between Larmor radius and probe width shown in Fig.9.

Figure 10 illustrates the distribution of electrons and ions at different magnetic fields. This clearly shows that the magnetic field influences the spatial distribution of electrons and ion.

4. Conclusion

We performed two dimensional PIC simulations in magnetized plasmas to analyze electron sheath formation. The effect of the geometry of the plane probe as well as the magnetic field of the probe on the electron sheath formation was analyzed.

The results revealed that changing the geometry of the plane probe from rectangular to square resulted in a decreases in sheath thickness and a close to CL sheath in the cylindrical geometry. Furthermore, the simulation results showed that the angular momentum of an electron, in case of low aspect plane probe, contributes to shield the electric field and decrease sheath thickness. This indicates that a cylindrical effect is dominates in a low aspect ratio plane probe.

Moreover, as illustrated in Fig.8, the effect of magnetic field on sheath formation was shown to depend on the relative relationship between the probe width and the Larmor radius of the electron.

Acknowledgements

One of the authors (K.A) wishes to thank to Mr. D. Atkins of Japan NUS for useful comments.

5. References

[1] For example, P.C Stangeby, The Plasma Boundary of Magnetic Fusion Devices, Taylor &Fransis Group (2000).

[2] S. Kajita, S. Kado, A. Okamoto, and S. Tanaka, Phys. Rev. E **70**, 066403 (2004).

[3] S. Kajita, S. Kado, and S. Tanaka, Contrib. Plasma Phys. **46**, 373 (2006).

[4] J.P. Verboncoeur, A.B. Langdon, N.T. Gladd, Compt. Phys. Commun. **87**, 199 (1995).

[5] I. Langmuir and K.B. Blodgett, Phys. Rev. **22**, 347 (1925).